Article

Cell Reports

Stem Cell-Specific Mechanisms Ensure Genomic Fidelity within HSCs and upon Aging of HSCs

Graphical Abstract

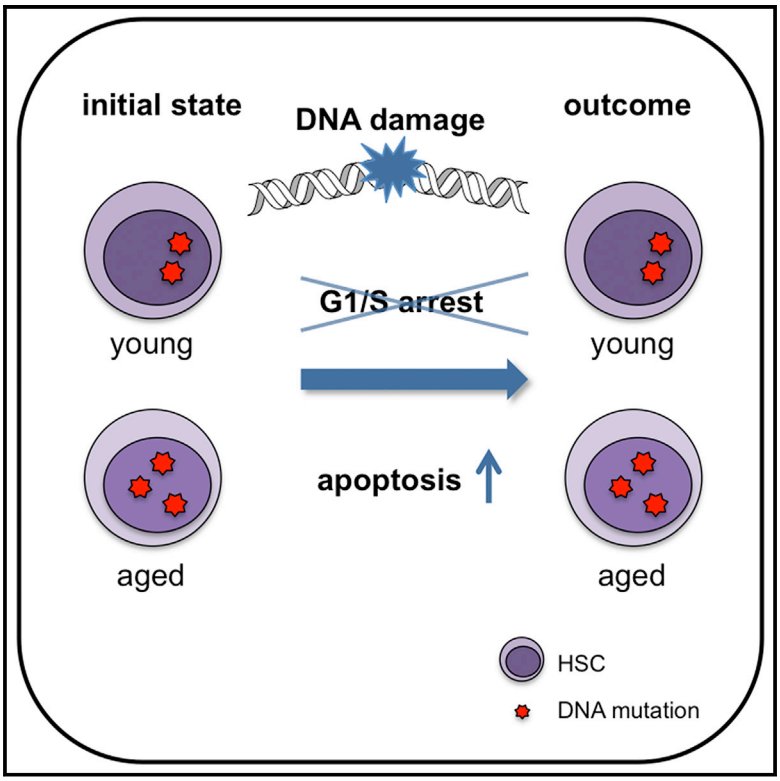

Authors

Bettina M. Moehrle, Kalpana Nattamai, Andreas Brown, ..., Peter Stambrook, Matthew Porteus, Hartmut Geiger

Correspondence

hartmut.geiger@uni-ulm.de

In Brief

Aged hematopoietic stem cells (HSCs) do not accumulate more mutations than young HSCs upon DNA damage. Moehrle et al. demonstrate that both young and aged HSCs lack a G1-S arrest and a high level of apoptosis upon DNA damage, rendering them resilient toward acquiring mutations upon DNA damage.

Highlights

- An aged hematopoietic system shows a 2- to 3-fold increase in DNA mutations
- The outcome of DNA damage is similar for young and aged HSCs
- Young and aged HSCs lack G1-S cell-cycle checkpoint activation upon DNA damage
- HSCs are resilient toward accumulating DNA mutations in response to DNA damage

Moehrle et al., 2015, Cell Reports *13*, 1–13
December 22, 2015 ©2015 The Authors
http://dx.doi.org/10.1016/j.celrep.2015.11.030

CellPress

Please cite this article in press as: Moehrle et al., Stem Cell-Specific Mechanisms Ensure Genomic Fidelity within HSCs and upon Aging of HSCs, Cell Reports (2015), http://dx.doi.org/10.1016/j.celrep.2015.11.030

Cell Reports
Article

OPEN ACCESS
CellPress

Stem Cell-Specific Mechanisms Ensure Genomic Fidelity within HSCs and upon Aging of HSCs

Bettina M. Moehrle,[1] Kalpana Nattamai,[2] Andreas Brown,[1] Maria C. Florian,[1] Marnie Ryan,[2] Mona Vogel,[1] Corinna Bliederhaeuser,[1] Karin Soller,[1] Daniel R. Prows,[3] Amir Abdollahi,[4,5] David Schleimer,[2] Dagmar Walter,[6] Michael D. Milsom,[6,7] Peter Stambrook,[8] Matthew Porteus,[9] and Hartmut Geiger[1,2,*]

[1]Institute of Molecular Medicine, University of Ulm, 89081 Ulm, Germany
[2]Division of Experimental Hematology and Cancer Biology, Cincinnati Children's Hospital Medical Center and University of Cincinnati, Cincinnati, OH 45229, USA
[3]Division of Human Genetics, Cincinnati Children's Hospital Medical Center and University of Cincinnati, Cincinnati, OH 45229, USA
[4]German Cancer Consortium (DKTK), 69120 Heidelberg, Germany
[5]Molecular and Translational Radiation Oncology, Heidelberg Ion Therapy Center (HIT), 69120 Heidelberg, Germany
[6]Heidelberg Institute for Stem Cell Technology and Experimental Medicine gGmbH (HI-STEM), 69120 Heidelberg, Germany
[7]Deutsches Krebsforschungszentrum (DKFZ), Division of Stem Cells and Cancer, Experimental Hematology Group, 69120 Heidelberg, Germany
[8]Department of Molecular Genetics, University of Cincinnati College of Medicine, Cincinnati, OH 45229, USA
[9]Department of Pediatrics, Stanford University, Stanford, CA 94305, USA
*Correspondence: hartmut.geiger@uni-ulm.de
http://dx.doi.org/10.1016/j.celrep.2015.11.030

SUMMARY

Whether aged hematopoietic stem and progenitor cells (HSPCs) have impaired DNA damage repair is controversial. Using a combination of DNA mutation indicator assays, we observe a 2- to 3-fold increase in the number of DNA mutations in the hematopoietic system upon aging. Young and aged hematopoietic stem cells (HSCs) and hematopoietic progenitor cells (HPCs) do not show an increase in mutation upon irradiation-induced DNA damage repair, and young and aged HSPCs respond very similarly to DNA damage with respect to cell-cycle checkpoint activation and apoptosis. Both young and aged HSPCs show impaired activation of the DNA-damage-induced G1-S checkpoint. Induction of chronic DNA double-strand breaks by zinc-finger nucleases suggests that HSPCs undergo apoptosis rather than faulty repair. These data reveal a protective mechanism in both the young and aged hematopoietic system against accumulation of mutations in response to DNA damage.

INTRODUCTION

Hematopoietic stem cells (HSCs) are tissue-specific stem cells that reside in the bone marrow (BM) and ensure the lifelong production of blood cells. This is achieved by the ability of HSCs to differentiate into a variety of specialized cells and to self-renew to achieve tissue homeostasis. HSC function declines from adulthood to old age, which contributes hematopoiesis dysfunction in older adults. Aging of HSCs and the hematopoietic system is characterized by senescence-associated immune remodeling and anemia (Van Zant and Liang, 2012; Geiger et al., 2013). Aged HSCs exhibit reduced self-renewal activity and a deficiency in their ability to produce erythrocytes and show a bias toward the myeloid lineage (Linton and Dorshkind, 2004; Signer and Morrison, 2013). Furthermore, aged HSCs present with a distinct gene expression signature and apolar distribution of proteins compared to young HSCs (Chambers et al., 2007; Florian et al., 2012).

The paradigm of the DNA damage theory of stem cell aging states that aging-associated changes in the DNA repair system in HSCs, together with changes in cell-cycle regulation due to increased DNA damage with age (Pietras et al., 2011; Rossi et al., 2007a), are thought to result in elevated DNA mutations, which then causally contribute to the decrease in HSC function with age. The paradigm is in part based on the finding that mice lacking a distinct set of DNA damage repair proteins display reduced function of HSCs, including an impaired repopulating potential and an overall depletion of the HSC pool (Ito et al., 2004; Navarro et al., 2006; Nijnik et al., 2007; Parmar et al., 2010; Prasher et al., 2005; Reese et al., 2003; Rossi et al., 2007a; Ruzankina et al., 2007; Zhang et al., 2010; Geiger et al., 2013), although in naturally aged mice, there is actually an expansion of the number of phenotypic stem cells instead of a depletion of the HSC pool. HSC aging also correlates with an increase in DNA double-strand breaks (DSBs). Both human and mouse HSCs present upon aging with a 2- to 3-fold elevated number of γH2AX foci, a bona fide surrogate marker for unresolved DSBs (Rossi et al., 2007a; Rübe et al., 2011). Unresolved DSBs accumulated in quiescent, but not cycling, HSCs upon aging (Beerman et al., 2014). γH2AX foci though were very recently shown to co-localize in HSCs with proteins associated with replication and ribosomal biogenesis stress (Flach et al., 2014), rendering γH2AX foci as a general marker for persistent DNA DSBs in HSCs questionable.

Signaling cascades activated in HSCs in response to DNA damage will determine the ultimate outcome of the damage.

Please cite this article in press as: Moehrle et al., Stem Cell-Specific Mechanisms Ensure Genomic Fidelity within HSCs and upon Aging of HSCs, Cell Reports (2015), http://dx.doi.org/10.1016/j.celrep.2015.11.030

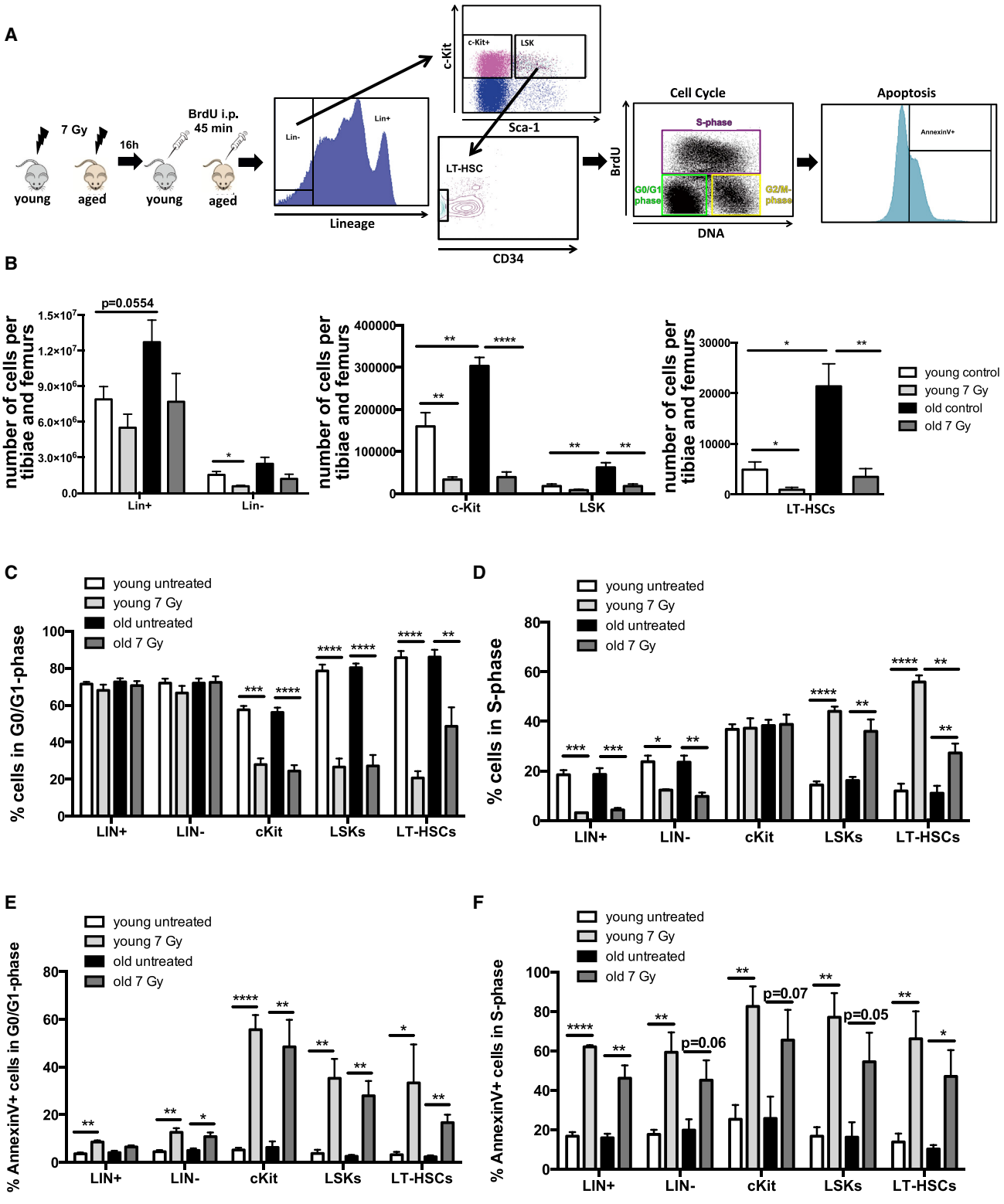

Figure 1. Distinct DNA Damage Checkpoint Activation Dynamics in Young and Aged HSCs upon Irradiation

(A) Experimental setting and gating strategy. Young (2–3 months) and aged (18–24 months) C57Bl6 mice were irradiated with 3 or 7 Gy. After 16 hr, 500 μg BrdU per mouse was injected intraperitoneally, and the mice were sacrificed 45 min later. BM was isolated and lineage$^-$ cells, c-Kit$^+$ cells, LSK cells, and LT-HSCs were analyzed by flow cytometry. Each population was scanned for cell-cycle status (BrdU incorporation over DNA content) and apoptosis (Annexin V$^+$).

(legend continued on next page)

The cascades might run in parallel, comprising initiation of DNA repair (intact or erroneous repair), apoptosis as well as senescence and differentiation signaling. DNA double-strand breaks (DSBs) can also be very potent inducers of cellular senescence in murine and human fibroblasts and murine HSCs (Di Leonardo et al., 1994; Nakamura et al., 2008; Shao et al., 2014). Differentiation in response to DNA damage has been described for various tissues including HSCs, melanocytic stem cells and embryonic stem cells (Inomata et al., 2009; Li et al., 2012; Wang et al., 2012). DNA damage induces apoptosis by p53-dependent and p53-independent pathways, and in lymphocytes and germ cells for example apoptosis represents the primary response to DNA damage (Lee et al., 1998). In murine HSCs, DNA damage induced by telomere attrition or DNA DSBs leads to an induction of lymphoid differentiation (Wang et al., 2012). Quiescent murine hematopoietic stem and progenitor cells (HSPCs) that are mostly residing in G0 phase of the cell cycle are thought to undergo an error-prone NHEJ pathway to repair DSBs (Mohrin et al., 2010). Upon irradiation, HSCs enter the cell cycle via elevation of p21, which implies that HSCs might use an error-free homologous recombination (HR) pathway to repair DNA damage (Insinga et al., 2013; Beerman et al., 2014). However, the outcome of DNA damage in HSCs with respect to mutational load upon damage resolution as well as stem cell function in correlation to aging has not been investigated in great detail.

In this study we therefore investigated DNA damage outcomes of aged and young HSPCs in more detail. Aging resulted in a 2- to 3-fold increase of the mutational load in the hematopoietic system. DNA damage response and outcomes in response to irradiation or chronic individual DSBs in young and aged HSCs though were similar. HSCs, both young and aged, were also very resilient toward further accumulation of DNA mutations in response to damage, which might be linked to unexpected differences in the DNA damage response between HSCs and differentiated cells regarding G1/S cell-cycle checkpoint activation. Collectively, we show that differentiated cells and HSCs respond differently to DNA damage, while the response is very similar for young and aged HSCs with respect to mutation accumulation and fitness in response to DNA DSBs.

RESULTS

Distinct DNA Damage Checkpoint Activation in HSCs upon Irradiation

DNA damage induces cell-cycle checkpoints as well as apoptosis, which are critical signaling cascades that directly impact DNA damage outcomes (Kastan and Bartek, 2004). Murine embryonic fibroblasts (MEFs), cell lines, and differentiated primary cells activate a G1/S cell-cycle checkpoint upon DNA damage through inhibition of the transcription factor E2F by the retinoblastoma (Rb) repressor complex. This results in a transcriptional arrest and a halt of progression into S phase and is regarded as a hallmark of the DNA damage response. Interestingly, embryonic stem cells skip activation of the G1/S checkpoint upon DNA damage (Aladjem et al., 1998; Hirao et al., 2000; Hong and Stambrook, 2004). We thus first asked which DNA-damage checkpoints are active in HSCs and whether at stage of checkpoint activation HSCs undergo apoptosis in response to DNA damage. To this end, flow cytometry assays to measure cell-cycle profiles and at the same time apoptotic status of young and aged HSPCs and differentiated hematopoietic cells were performed 16 hr after in vivo irradiation (Figure 1A). In response to 7 Gy (sublethal) irradiation, the total number of young and aged hematopoietic progenitor cells (c-Kit$^+$ cells), early hematopoietic progenitor cells (LSK cells), and long-term repopulating HSCs (LT-HSCs), but not yet that of terminally differentiated (Lin$^+$) cells (Figure 1B), was significantly reduced. These data are consistent with a positive correlation between radiation sensitivity and primitiveness of hematopoietic cells.

Differentiated hematopoietic cells (Lin$^+$ as well as Lin$^-$ cells) presented with the same frequency of cells in G0/G1 upon irradiation, while more primitive young as well as aged c-Kit$^+$, LSK, or LT-HSCs showed a lower frequency of cells in G0/G1. This implies an impaired activation of the G1-S checkpoint in primitive hematopoietic cells (PHCs) (Figures 1C and 1D). All cell types accumulated to a similar extent in the G2/M phase upon irradiation, implying a functional G2/M or mitotic checkpoint (Figure S1A). The impaired activation of the G1-S checkpoint was not restricted to the C57BL/6 strain (HSCs from DBA/2 mice show a similar phenotype) and can already be observed at lower doses of irradiation (Figures S1C, S1D, and S2C). An impaired activation of the G1-S restriction checkpoint upon DNA damage was further implied by the finding that the frequency of HSPCs (c-Kit$^+$, LSK, and LT-HSCs) in S phase of the cell cycle increases upon irradiation (Figure 1D).

Loss of the retinoblastoma (Rb) protein in fibroblasts results in a loss of a G1-S checkpoint activation and genetic instability (van Harn et al., 2010). A lack of G1-S activation in HSPCs would thus render Rb in HSCs dispensable with respect to the DNA damage response. We therefore tested activation of DNA damage signaling in hematopoietic cells deficient for Rb (Rb HemKO; Daria et al., 2008). Consistent with our prediction, HSPCs devoid of Rb did not show any difference in checkpoint activation upon irradiation nor in the number of γH2AX foci or tail length in a comet assay, another surrogate assay for DNA strand breaks (Figures S2A–S2C). However, we observed a small but significant increase of cells in S-phase of the cell cycle in steady state in Rb HemKO mice (Figure S2C), supporting a role for Rb in regulation of the G1/S checkpoint in HSPCs with respect to basic proliferation.

(B) Total number of Lin$^+$, Lin$^-$, c-Kit$^+$, LSK, and LT-HSC cells per tibiae and femur determined by flow cytometry 16 hr after total body irradiation with 7 Gy. *p < 0.05, **p < 0.005, ***p < 0.001, ****p < 0.0001; columns represent means +1 SEM; n = 5.
(C and D) Percentage of cells in either G0/G1 or S phase of the cell cycle. *p < 0.05, **p < 0.01, ***p < 0.001, ****p < 0.0001 statistics relative to control group; columns represent means +1 SEM; young control n = 5, young 7 Gy n = 3, old control n = 5, old 7 Gy n = 5.
(E and F) Percentage of Annexin V$^+$ cells either in G0/G1 or S phase of the cell cycle. *p < 0.05, **p < 0.01, ***p < 0.001, ****p < 0.0001 statistics relative to control (columns represent means +1 SEM); young control n = 5, young 7 Gy n = 3, old control n = 5, old 7 Gy n = 5.
See also Figure S1.

Please cite this article in press as: Moehrle et al., Stem Cell-Specific Mechanisms Ensure Genomic Fidelity within HSCs and upon Aging of HSCs, Cell Reports (2015), http://dx.doi.org/10.1016/j.celrep.2015.11.030

Activation of the G1-S checkpoint is supposed to stop a cell from entering S phase of the cell division cycle to allow for DNA repair processes in G0/G1, which in turn inhibit apoptosis initiated by the DNA damaging event (Sancar et al., 2004). Our analyses revealed that differentiated hematopoietic cells showed low levels of apoptosis in G0/G1 phase in response to irradiation and elevated levels in the S and G2-M stages of the cell division cycle (Figures 1E, 1F, and S1B). Surprisingly, there was already a strong induction of apoptosis in G0/G1 in more primitive cells (c-Kit$^+$, LSK, and LT-HSCs) in response to irradiation, with levels of apoptosis remaining high in S and G2-M. This indicated that HSPCs undergo apoptosis in response to irradiation, independent of their cell-cycle checkpoint position.

The lack of G1-S checkpoint activation correlated with very low levels of expression of the checkpoint kinase Chk2 (critical for G0/G1 checkpoint activation) in HSPCs upon irradiation (data not shown) as well as sequestration of Chk2 to the Pericentrin-2-positive centrosome in primitive hematopoietic cells, most likely rendering Chk2 ineffective (Figure S2D). Elevated expression of Chk2 in hematopoietic cells activated a G0/G1 arrest upon DNA damage while maintaining the relatively high level of apoptosis already seen in G0/G1. This resulted in impaired stem and progenitor cell function in transplantation assays (Figures S2E–S2G), which was dependent on the kinase function of Chk2. These data imply that induction of Chk2 expression activates a G0/G1 checkpoint in HSPCs at the expense of a high level of apoptosis upon DNA damage (see Figures 1E and 1F). In summary, young as well as aged HSPCs actively suppress activation of the G1-S checkpoint upon irradiation and present at the same time with high levels of apoptosis upon DNA damage, independent of their position within the cell division cycle.

Robust Protection of Genomic Integrity in Young and Aged HSCs

Various reports indicate persistence of DNA damage after irradiation in HSCs and elevated steady-state damage in aged HSCs (Rossi et al., 2007b; Mohrin et al., 2010; Insinga et al., 2013) or elevated levels of stalled replication forks (Flach et al., 2014). We therefore determined the frequency of γH2AX foci in response to irradiation in young and aged LT-HSCs, which has been regarded as a surrogate marker for the frequency of DSBs in the genome. Aged LT-HSCs presented with a small, but significant increase in the number of foci per cell as also previously reported (Beerman et al., 2014; Flach et al., 2014; Rossi et al., 2007a) (Figure S3A). The comet assay quantifies changes in DNA migration caused by DSBs, alkaline labile sites, and transient repair sites. Aged LT-HSCs presented with a minor elevated tail moment under steady-state conditions compared to young cells (Figure S3B) (see also Beerman et al., 2014). Both young and aged LT-HSCs presented with a similar absolute increase in the tail moment as well as γH2AX foci number after irradiation. Interestingly, theses changes were not linked to oxidative stress, since levels of 8-oxo-dG (a quantitative marker of oxidative damage of DNA) did not show significant differences between young and aged LT-HSCs in steady state and after irradiation (Figure S3C).

We also determined the loss of heterozygosity (LOH) at distinct microsatellite marker locations to further quantify the outcome of DNA damage. Monoclonal colonies (from a CFC assay) derived from individual young and aged hematopoietic progenitor (LK cells) as well as early hematopoietic progenitor cells (LSK cells) presented with similar LOH frequency. Upon irradiation at 5 Gy ex vivo, aged LSK presented with a 2- to 3-fold increase in the LOH frequency compared to young LSK cells (Table S1). The CFC assay is performed under supraphysiological cytokine conditions, which have been reported to suppress apoptosis in hematopoietic cells upon irradiation (Chute et al., 2004; Hérodin and Drouet, 2005). The extent in increase in LOH frequency is similar in magnitude to the increase, for example, in tail moment of aged HSCs in the comet assay (Figure S3B).

To test whether DNA damage will alter stem cell function in vivo distinctly in young and aged HSPCs, competitive transplantation/irradiation/recovery experiments were performed in which young and aged HSCs directly functionally compete post-DNA-damage in the same recipient animal. Functionality of young and aged HSCs is indicated by the level of chimerism of donor cells in peripheral blood 3 months post-irradiation. We detected almost identical chimerism ratios of old (Ly5.2$^+$) versus young cells (remaining cells, Ly5.1$^+$) in control versus irradiated animals (Figures 2A and 2B), strongly implying that stem cell function upon irradiation is very similar in young and aged HSCs. This conclusion is further supported by our finding that young and aged stem and progenitor cells showed almost identical survival frequencies upon irradiation in various functional in vitro assays (cobblestone-area-forming cell [CAFC] assay as well as colony-forming cell assays; data not shown).

Using a validated and widely accepted transgenic plasmid based mutation detection assay (Figure 2C) (Boerrigter et al., 1995; Geiger et al., 2006, 2009), we next analyzed DNA repair outcomes in hematopoiesis with respect to fidelity of the DNA damage repair process in vivo by determining mutation frequencies in response to DNA damage. Mutation frequencies in BM cells from transgenic mice were determined in response to total body irradiation (3 Gy) 4 days (resembling activity of differentiated cells), 28 days (indicative of progenitor cell activity), and 3 months (hematopoiesis indicative of HSCs activity) after irradiation. BM cells in aged mice had a trend toward an increased mutational load in steady-state hematopoiesis (~2-fold) (Figure 2D). The majority of mutations detected were translocations and/or deletions (data not shown) and not point mutations, which is a unique pattern of mutations among all tissues analyzed so far with this indicator strain (Dollé et al., 2000). Surprisingly, the mutation frequency in BM cells did not increase in response to irradiation. To the contrary, the mutation frequency significantly decreased 28 days postirradiation in BM cells as well as at 3 months post-irradiation in both age groups, with translocations still being the majority of the remaining mutations (Figure 2D and S3D). This implies that the DNA damage response of the hematopoietic system avoids accumulation of genomic mutations upon irradiation and this mechanism remains fully intact in aged animals. The data also demonstrate that young and aged HSPCs show a similar in vivo response to DNA damage and a similar DNA damage repair outcome in response to irradiation, with an overall low mutational load.

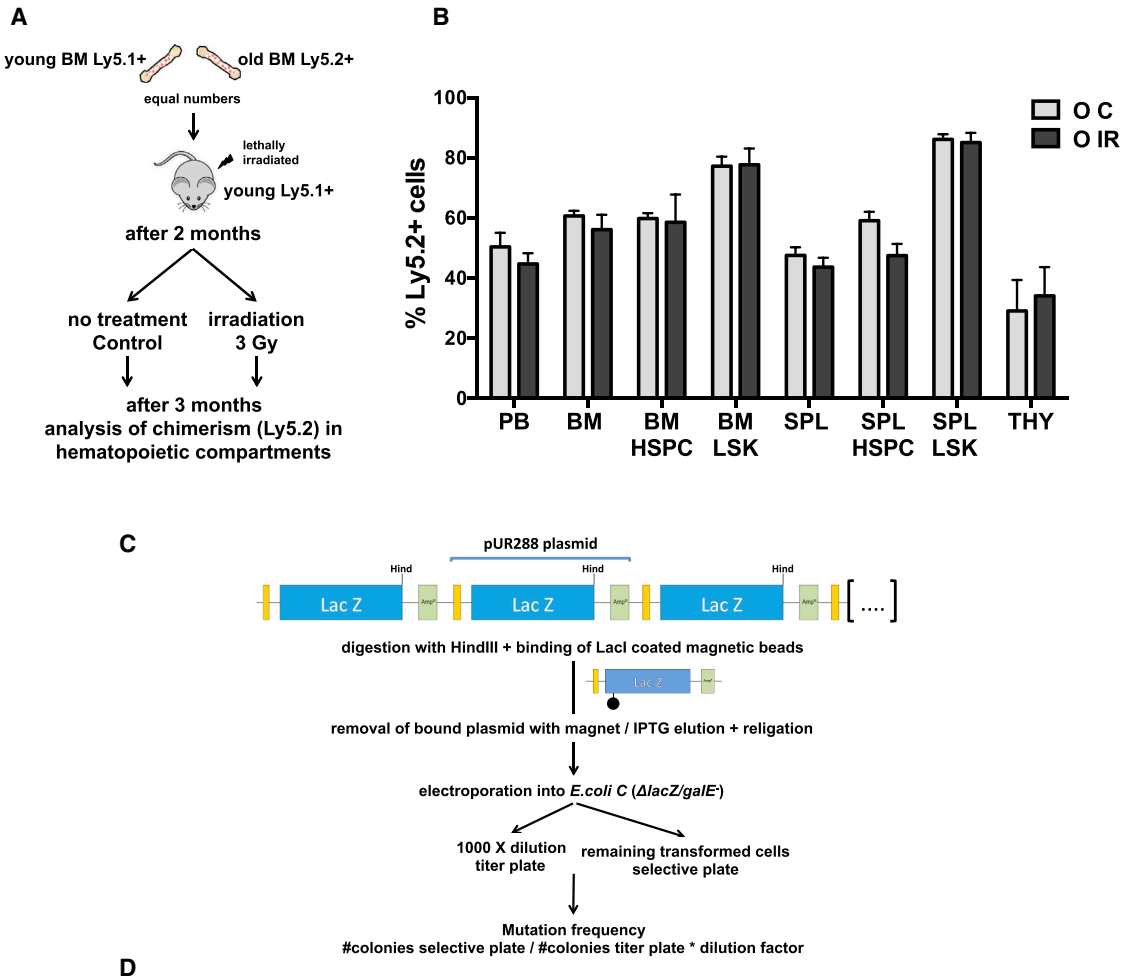

Figure 2. Protection of Genomic Integrity in Young and Aged Hematopoietic Cells upon DNA Damage In Vivo

(A) Schema of experimental setup.

(B) Chimerism of Ly5.2$^+$ cells within the different hematopoietic compartments. Control n = 5, 3 Gy n = 7; PB, peripheral blood; BM, bone marrow; SPL, spleen, THY, thymus, LSK, lineage-negative/c-Kit$^+$/Sca-1$^+$ BM cells; HSPC, hematopoietic stem and progenitor cells. Columns represent means +1 SEM. See also Figure S2.

(C) Experimental setup of the assays to determine genomic mutations (see Experimental Procedures for details).

(D) Mutation frequency (number of mutated plasmids per 10^4 plasmids analyzed) of BM cells derived from young (2–3 months) and aged (18–24 months) mice before and 4 days, 28 days, and 3 months after irradiation with 3 Gy. n = 18 for young, n = 5 for aged, n = 7 for young (90 days), n = 5 for aged 90 days, n = 3 for young (4 days, 28 days) and aged 28 days, and n = 2 for aged 4 days; *p < 0.05, **p < 0.01, ****p < 0.0001 (compared to values after 4 days within group), §p < 0.05, §§p < 0.05 (compared to values before irradiation within group), $^{\#}$p = 0.0524 (Y compared to O); columns represent means +1 SEM.

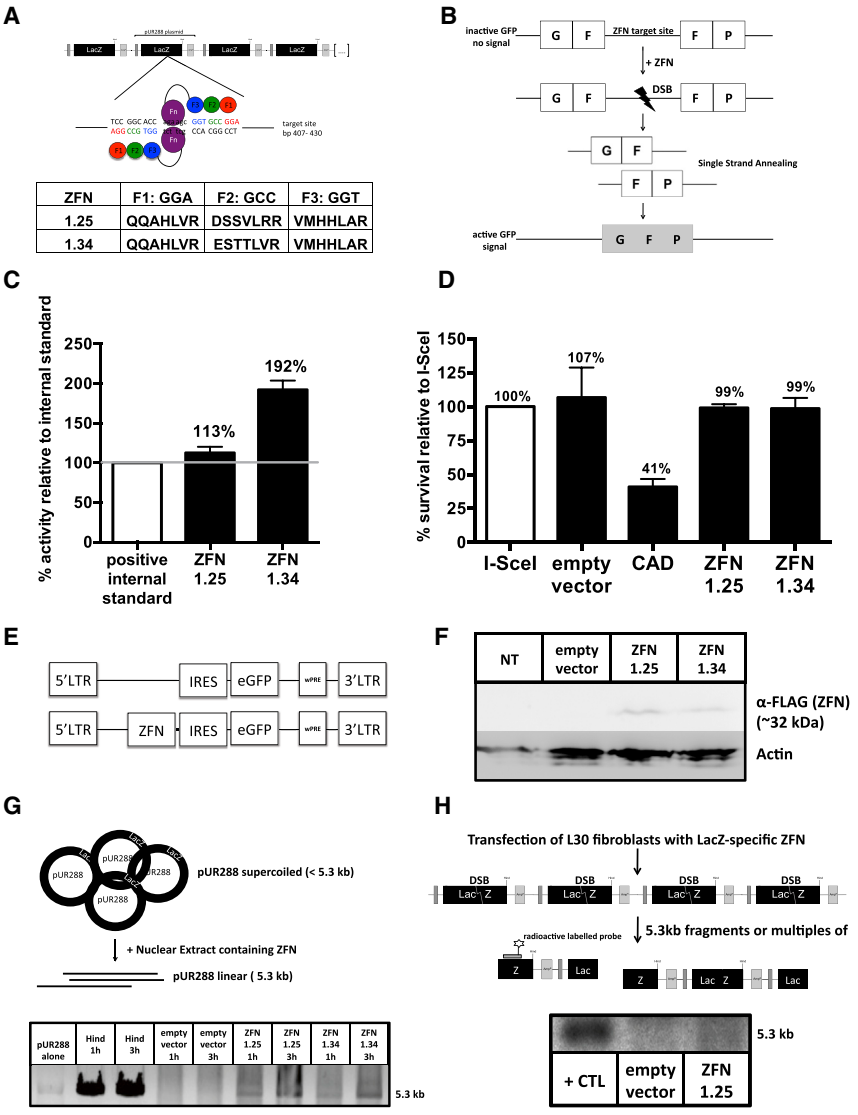

ZFN	F1: GGA	F2: GCC	F3: GGT
1.25	QQAHLVR	DSSVLRR	VMHHLAR
1.34	QQAHLVR	ESTTLVR	VMHHLAR

Figure 3. Confirmation of In Vivo Activity of a *lacZ*-Specific Zinc-Finger Nuclease

(A) Each three-finger zinc finger (F1, F2, and F3) linked to the FokI nuclease domain (zinc-finger nuclease [ZFN] binds to a 9-bp half of a palindromic pUR288 plasmid target site. The amino acid sequences of the zinc-finger domains (F1, F2, F3) of the two ZFNs (1.25 and 1.34) are depicted.

(B) Schematic representation of the SSA assay. In the assay, the activity of the ZFN is proportional to the expression of GFP.

(C) Activity of the ZFNs relative to a positive standard. n = 3. Columns represent means +1 SEM.

(D) ZFN toxicity assay: survival of fibroblasts co-transfected with a GFP plasmid and either with the ZFN or with the non-toxic endonuclease I-Sce-I (negative control) or caspase-activated DNase (CAD, positive control), n = 3. Columns represent means +1 SEM.

(E) Gammaretroviral bicistronic SF91/ZFN-IRES-eGFP vector used for stable transduction of cells (LTR, long terminal repeat with strong enhancer element; wPRE, woodchuck hepatitis virus post-transcriptional regulatory element).

(F) Expression of the ZFNs 1.25 and 1.34 and actin in fibroblasts transduced with the SF91/ZFN-IRES-eGFP vector (representative western blot).

(G) Schematic representation of experimental setup. Agarose gel electrophoreses of pUR288 plasmid incubated with nuclear extracts for 1 or 3 hr from cells transduced with the SF91/ZFN-IRES-eGFP virus containing the ZFNs, pUR288 alone (negative control) and pUR288 digested with the restriction enzyme HindIII (positive control).

(H) Schematic representation of experimental setup. Representative southern blot against pUR288. CTL, genomic DNA digested with HindIII (positive control). The linear plasmid has a size of 5.3 kb.

In summary, both young and aged PHCs strongly avoid having DNA-damaged cells in the G0/G1 state. They present with a high level of apoptosis upon DNA damage induced by irradiation and show for a selective type of DNA mutations (LOH) in response to in vitro damage a 2- to 3-fold increase, while DNA-damage-surviving cells in vivo do not accumulate DNA mutations as determined by the indicator strain. These data imply a mechanism of either repair with an overall low error rate or a strong selection for undamaged cells. Also, clearing of damaged cells that exceed a threshold for a still-tolerated mutation number or induction of replicative senescence might contribute to this outcome. This suggests that the hematopoietic system is actively managing the DNA damage response outcome in vivo with respect to mutational load.

Generation of a Defined DNA DSB In Vivo in Stem Cells via a *lacZ*-Specific Zinc-Finger Nuclease

We further tested this "reduce the mutational load upon damage" hypothesis of PHCs in vivo. Specifically, a defined DSB was induced by homodimeric zinc-finger nucleases (ZFNs) (we generated two distinct ZFNs versions, 1.25 and 1.34; Figure S4A) specific to a palindromic target site within the *lacZ* gene (at bp 407–430; Figure 3A) (Maeder et al., 2009). ZFNs bind as dimers to their specific target site (in our case *lacZ*, transgenic mouse) and a DNA DSB is generated via the attached Fok1 nuclease within the spacer region (6 bp), separating the two binding domains (9 bp each; Figure 3A). A plasmid-based single-strand annealing repair assay in which the activity of the ZFN is proportional to the expression of GFP (Porteus and Baltimore, 2003) demonstrated increased activity of the zinc fingers relative to standard controls (113% for 1.25 and 192% for 1.34; Figures 3B and 3C). A cell survival assay, in which the nontoxic endonuclease I-SceI from yeast was used as a negative standard for reference and transfection with caspase-activated DNase (CAD) served as positive control, revealed no toxicity of the zinc fingers and thus no unspecific off-target activity (Figure 3D). Transfection with ZFNs did not result in a significantly elevated number of γH2AX foci in cells containing no *lacZ* target site (data not shown), further confirming specificity of the ZFNs for their target site. For stable

expression of the ZFNs in cell lines and HSCs, a bicistronic retroviral vector SF91/ZFN-IRES-eGFP was used (Figure 3E). Expression of ZFN proteins was confirmed by western blotting of cells transduced with the ZFNs (Figure 3F). To further determine activity in vivo, we next investigated the activity of nuclear extracts from eGFP$^+$ fibroblast cells transduced with the ZFNs on purified pUR288 plasmid containing the *lacZ* target sequence. Incubation of the plasmid for 1 hr with the nuclear extract resulted in linearization of the plasmid (5.3-kb band), which intensified in response to a 3-hr incubation, confirming specific ZFN activity in nuclear extracts (Figure 3G). In order to verify activity on genomic *lacZ* DNA in vivo, DNA from *lacZ* murine (small blue mouse) cells, which were transfected with the ZFN 8 hr prior to analysis by Southern blot, was used. Since the pUR288 plasmid is integrated as a concatemer of 20 copies within the genome, the creation of a DNA DSB at the ZFN target site in vivo will result in DNA fragments the size of the plasmid (5.3 kb) (Figure 3H). ZFN 1.25 displays a distinct band at 5.3 kb, which is a unique result as usually "free" degradation products of ZFNs in vivo are very difficult to track due to their short half-life in vivo. In summary, the two ZFNs generated are active on *lacZ*-DNA in vivo and specific and thus are a unique tool to determine the response of stem cells to defined DSBs.

Young and Aged HSCs Sense Single DSBs to Protect Their Genome

ZFN transduced and subsequently sorted (eGFP$^+$) Lin$^-$ BM cells from the *lacZ* transgenic mouse were expanded in vitro for 3 days prior to analysis to obtain the cell numbers and thus the amount of DNA necessary for the mutation assay (Figure S4B). Lin$^-$ BM cells transduced with the *lacZ*-specific ZFNs showed a slight non-significant increase in the mutation frequency (Figure S4B). This finding implies a resilience of these cells to acquire DNA mutations, and it correlates with the fact that PHCs do not activate a G1/S checkpoint and might thus avoid repair in G0/G1 and the DNA repair program associated with G0/G1. Mutation frequencies in PHCs are very difficult to determine due to the amount of DNA necessary for the assay. We instead focused on functional assays for *lacZ*-positive HSCs transduced with ZFNs. Transduced Lin$^-$ cells (eGFP$^+$) from young and aged mice were transplanted into lethally irradiated recipient mice (Figure 4A). 18–21 weeks after transplantation, when hematopoiesis in the periphery is driven by transplanted HSCs, ZFN-positive young as well as aged HSCs presented with as significant decrease in eGFP$^+$ cells among donor cells in PB and BM (Figures 4B and 4C). The fitness/status though of the transplanted HSPCs was not altered right after transduction, as there was no difference in the frequency of colony-forming activity between control and ZFN-transduced cells (Figure S4C). Because the active ZFN will constantly target the *lacZ* locus in stably transduced cells, a likely outcome is that almost all "surviving" eGFP$^+$ clones show mutations in *lacZ*. Surprisingly, but consistent with the data presented so far, the remaining small number of eGFP$^+$ transduced cells that could be recovered from the BM after transplantation did present with only a very low number of DNA mutations within the transgene (one single clone with a point mutation at the ZFN target site in one mouse transplanted with aged Lin$^-$ cells; Figure 4D).

Our data therefore demonstrate that HSCs are resilient against acquiring mutations upon DNA damage in vivo, implying a ridged quality control mechanism to preserve genomic integrity of the stem cell pool. Interestingly, this approach and its underlying mechanisms are not altered upon aging of the hematopoietic system.

DISCUSSION

The loss of maintenance of genomic integrity is central to most theories on somatic and stem cell aging. Analysis of HSCs with respect to the frequency of DNA damage (comet assay, γH2AX foci, DNA mutation frequency, LOH assay) revealed an ~2- to 3-fold increase in these parameters upon aging. The difference in mutation frequency in steady state between young and aged BM cells was ~2-fold, which is in the range of changes in mutation frequencies recently reported for aged human BM cells via deep-sequencing approaches (Cancer Genome Atlas Research Network, 2013; Genovese et al., 2014; Welch et al., 2012). In a diploid genome that harbors ~6×10^9 nt, the total estimated mutational load per diploid BM cell is then ~300 mutations in young and ~600 mutations in an aged animals. Whether such an increase upon aging is causatively linked to aging-associated diseases though still needs to be determined. A 22-fold increase in the mutational load (Geiger et al., 2006) is able to initiate leukemia in a mutator gene type setting (Kushner et al., 2008; Noronha et al., 2006; Su et al., 2005), while a 2- to 3-fold mutation load increase in BM cells does not induce leukemia (Krejci et al., 2008). The concept of a robust response of aged stem cells to DNA damage is further supported by the finding that muscle stem cells do not present with a significant accumulation of DNA damage upon aging (Cousin et al., 2013).

Might the elevated γH2AX foci and increased tail moment in comet assays upon aging also be linked to aging-associated changes in stem cells other than just DNA damage? In murine hair follicle stem cells, 53BP1 foci, a mechanistic marker for DNA DSBs, did not overlap with γH2AX foci, and instead γH2AX foci were identified as a sign for chromatin alterations upon aging (Schuler and Rübe, 2013). Very recently, it was shown that elevated levels of γH2AX foci in aged HSCs can be also associated with replication and ribosomal biogenesis stress and might therefore not be an optimal marker for persistent DNA damage (Flach et al., 2014). Instead, elevated levels of γH2AX foci in aged HSCs might be linked to broader chromatin changes, which can, but need not to be, linked to DNA damage (Florian et al., 2012; Liu et al., 2013) Such changes might be linked to migration velocity of DNA in assays like the comet assay. Furthermore, it was shown by Beerman et al. (Beerman et al., 2014) that quiescent HSCs acquire DNA damage upon aging, but when these cells are pushed into the cell cycle, the damage is repaired. Our data suggest a mechanistic explanation for this finding, demonstrating that aged cells with DNA damage are pushed into the cell cycle and either repair properly without mutations or simply die.

In summary, we demonstrate that both young and aged HSCs that survive irradiation are repaired properly with a low mutation rate regardless of their age. Our data strongly imply that both the young and aged hematopoietic systems are very resilient toward

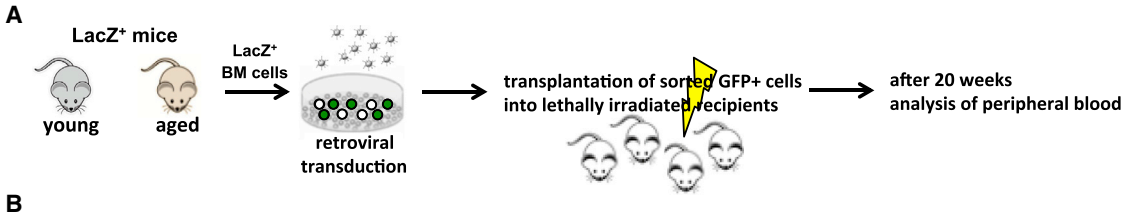

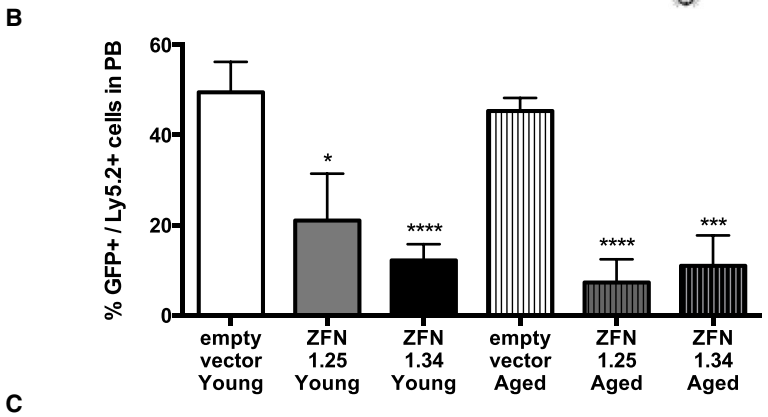

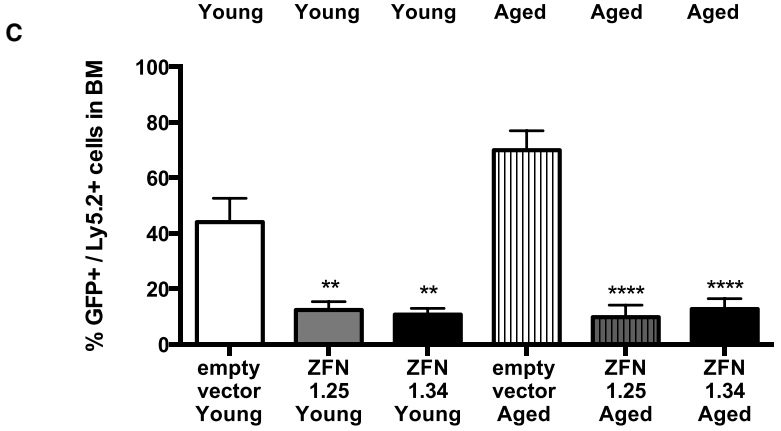

D

Young	clones analyzed	mutations @ target site
empty vector	15	0
ZFN 1.25	15	0
ZFN 1.34	17	0

Aged	clones analyzed	mutations @ target site
empty vector	15	0
ZFN 1.25	15	0
ZFN 1.34	18	1 (point mutation)

Figure 4. Young and Aged HSCs Sense Single DSBs and Protect Their Genome

(A) Experimental setup.

(B and C) Contribution of transduced cells ($GFP^+/Ly5.2^+$ cells) to peripheral blood (PB) and bone marrow (BM) 18–21 weeks after transplantation. *$p < 0.05$, **$p < 0.01$, ****$p < 0.0001$; columns represent means +1 SEM, n = 3 with a cohort of three to five recipient mice per group.

(D) Number of mutations in the *lacZ* ZFN target site sequence in GFP+ BM cells (clone) 18–21 weeks post-transplant.

acquiring mutations upon DNA damage induced by irradiation, trying to maintain a pristine pool of HSCs contributing to hematopoiesis and to strongly suppressing leukemia. How is this resilience achieved? Multiple cellular and molecular mechanisms seem to contribute to that. First, LT-HSCs are more sensitive to irradiation than their progeny as 3 Gy resulted in the loss of LT-HSCs whereas Lin^-, $c\text{-}Kit^+$, and LSK cells did not show a significant decrease in cell number (our own data; Mohrin et al., 2010). Second, and probably more importantly, our results show an unexpected loss of activation of the G1-S cell-cycle

checkpoint in HSPCs already at lower doses of irradiation (3 Gy), which was even more pronounced after high-dose irradiation. Such an observation is similar to what has been described for embryonic stem cells, which also show absence of a G1-S checkpoint upon damage (Aladjem et al., 1998; Hong and Stambrook, 2004). A lack of checkpoint activation in HSPCs was further supported by our finding that deletion of Rb in hematopoietic cells did not alter DNA damage response parameters. One alternative hypothesis, based on these observations, is that the genetic translocations and deletions found in leukemia cells are actually not a consequence of faulty repair by non-homologous end-joining (NHEJ) in G0/G1 and rather imply that translocations and deletions are generated via faulty repair mechanisms at later stages of the cell division cycle, like in S, G2, or M phase.

In fibroblasts, irradiation leads to a prolonged cell-cycle arrest in G1 phase to halt the cell for repairing DNA damage before entering the cell cycle (Deckbar et al., 2011; Di Leonardo et al., 1994), whereas the same challenge could also lead to apoptosis, senescence, or differentiation. In hematopoietic cells, we observed that differentiated cells that do arrest in G0/G1 phase did not undergo apoptosis, whereas more primitive cells did not arrest and showed high levels of apoptosis. Also, human $CD34^+$ HSPCs show increased apoptosis in response to DNA damaging agents when compared to differentiated cells (Buschfort-Papewalis et al., 2002). An elevated level of apoptosis in S phase is supported by the finding that HSPCs, when proliferating, present with a decreased expression of prosurvival genes compared to quiescent cells (Mohrin et al., 2010).

Murine embryonic stem cells also lack G1-S checkpoint activation, which is due to intracellular mislocalization of the checkpoint kinase Chk2 (Hong and Stambrook, 2004). In murine LT-HSCs, the Chk2 protein is not expressed throughout the nucleus, like in differentiated cells, but sequestered at the centrosome. Ectopic expression of Chk2 in HSCs reduced function of HSCs, which is consistent with our finding that primitive hematopoietic cells, when in G0/G1, respond primarily with apoptosis to DNA damage. Taken together, the most likely outcome of DNA damage in a primitive hematopoietic cell might be dual in nature: apoptosis or repair without mutations. Such a model might not only hold true for DNA damage found at multiple locations within the cell as in response to irradiation. Our results further demonstrate that PHCs transduced with a ZFN that will create one site of DSBs per cell do not show an increase in mutation frequency. When transplanted, we further demonstrate that these cells are unable to contribute to PB chimerism as they most likely undergo apoptosis or senescence.

In aggregation, our results demonstrate a 2- to 3-fold increase in the steady-state mutational load in the hematopoietic system but almost equal DNA damage repair outcomes in young and aged HSCs. The role for DNA damage outcomes with respect to aging of HSPCs will need to be further investigated. Most importantly, these data reveal a heretofore unrecognized resilience of the hematopoietic system in general to acquire DNA mutations in response to DNA damage in vivo.

EXPERIMENTAL PROCEDURES

Mice

C57BL/6 mice (8–12 weeks old and 18–26 months old) as well as C57BL/6.SJL-Ptprca/Boy (BoyJ) mice were obtained from Janvier or the divisional stock (derived from The Jackson Laboratory). L30 *lacZ*$^+$ mice (Tg(LacZpl)60Vij/J, small blue mouse, backcrossed on C57BL/6 background) were described previously (Boerrigter et al., 1995). Mice were housed under specific-pathogen-free conditions at the University of Ulm or at the Cincinnati Children's Hospital Medical Center (CCHMC). Experiments were performed in compliance with the German Law for Welfare of Laboratory Animals and were approved by the Regierungspräsidium Tübingen or the Institutional Animal Care and Use Committee at CCHMC.

Generation of a L30 *lacZ*$^+$ Adult Fibroblasts Cell Line

Fibroblasts of L30 *lacZ*$^+$ and *lacZ*$^-$ mice were generated as described before (Bosco and Knudsen, 2005). L30 *lacZ*$^+$ adult fibroblasts started to become immortalized between passages 11 and 15 and were then used for experiments.

Mutation Assay

The mutation frequency analysis using the L30/small blue mouse model was performed as previously described (Boerrigter et al., 1995; Dollé et al., 1997; Geiger et al., 2009; Vijg et al., 1997)

Determination of Loss of Heterozygosity upon DNA Damage via Analysis of Loss of Inbred Strain-Specific Microsatellites in B6D2F1 Mice

Clonal colonies (CFCs in complete methylcellulose medium, STEMCELL Technologies) from Lin^-, c-Kit^+ cells or Lin^-, c-Kit^+ Sac-1^+ cells from young (2–3 months) or aged (22 months old) B6D2F1 mice were picked between days 7 and 9, washed in PBS, and subsequently lysed (0.91 mg/ml Proteinase K, 0.5% Tween20, and 0.5% Nonidet P40). DNA was subjected to multiplex cocktails of fluorescently labeled primers that flank small tandem nucleotide repeats (microsatellites) polymorphic in length between DBA2 and B6. PCR amplified DNA (95°C 15 min; then 38 cycles of 94°C 30 s, 57°C 1:30 min and 72°C 1 min; 60°C 30 min, and 4°C forever) was analyzed by capillary electrophoreses, and peak calling relative to B6 and DBA/2 controls was performed with Gene Mapper software. (primers for LOH assay were picked randomly among the microsatellite markers that are distinct in length between C57BL/6 and DBA/2 and readable in multiplex setup while covering most chromosomes: D1Mit380, D9Mit123, DXMit64, D8Mit45, D12Mit143, D4Mit17, D16Mit60, D14Mit39, D3Mit57, D18Mit177, D10Mit230, D5Mit309, D2Mit66, D13Mit256, D19Mit96, D1Mit102, D6Mit284, D7Mit350, and D15Mit67).

Generation of *lacZ*-Specific Zinc-Finger Nuclease

The *lacZ*-specific ZFNs 1.25 and 1.34 were generated using the OPEN method (oligomerized pool engineering) (Maeder et al., 2009). The homodimeric ZFN target site within the *lacZ* (bp 407–430, 5′-TCCGGCACCAGAAGCGG TGCCGGA-3′) was identified using the web-based software provided by the ZFN consortium. Bacterial two-hybrid (B2H) selection strains were then constructed harboring the ZFN target half-sites upstream of a B2H promoter. The zinc-finger array libraries were constructed by using DNA sequences encoding fingers from preselected "pools" for each targeted triplicate (F1: GGA, F2: GCC, F3: GGT) that were fused together by overlap PCR (Porteus, 2008). This resulted in a library of DNA sequences encoding random combinations of fingers. These DNA sequences were then cloned into low-copy expression phagemids and converted into infectious phage particles that were used to infect B2H selection cells (kanamycin/tetracycline/sucrose selection). Phagemids encoding the zinc-finger arrays that bind to the target site were isolated from colonies on the selection plates, the zinc-finger array DNA sequence amplified by PCR reaction, fused to a five-amino-acid linker sequence, and ligated to the wild-type FokI nuclease domain. For sequences of *lacZ*-specific ZFNs, see Figure S4.

For expression of the ZFN in hematopoietic cells, the bicistronic retroviral vector SF91/IRES-eGFP was used. Cell-free supernatants containing retroviral particles were generated by transient transfection of Phoenix-gp

packaging cells (ATCC number CRL-3215) using Calcium Phosphate Transfection kit (Invitrogen).

Activity of ZFNs on Target Site: SSA Assay

The full ZFN target site was inserted into repeated sequences within the GFP gene. The reporter constructs also included the GFP1/2 full ZFN target site (5′-ACCATCTTC-ttcaag-GACGACGGC-3′) as a positive control and internal standard previously described by Pruett-Miller et al. (2008) as GFP1.4-B2H and GFP2-B2H. These SSA reporter plasmids were used to investigate the activity of the ZFNs on their target site. 100 ng of each ZFN-expression plasmid and 20 ng reporter plasmid were co-transfected into HEK293 or 293T cells using the calcium phosphate transfection kit (Invitrogen). Percentage of GFP^+ cells (DSB of ZFN at target site and subsequent SSA repair, restoring GFP expression) was determined at day 2 via flow cytometry. The activities of the ZFNs 1.25 and 1.34 were normalized to the activity of the internal standard.

Preparation of Nuclear Extract Harboring ZFNs

Nuclear extract was prepared from stably transfected L30 *lacZ*$^-$ fibroblasts with the SF91/ZFN-IRES-eGFP virus based on Dignam et al. (1983). Protein concentrations obtained were between 2 and 6 μg/μl.

Activity of ZFNs on pUR288 Plasmid: Plasmid Assay

2 μg supercoiled pUR288 plasmid were incubated at 37°C for 1 to 3 hr in 1× NEB buffer 2 with 50 μg nuclear extracts from cells transduced with the SF91/ZFN-IRES-eGFP virus and applied to a 1% agarose gel. Plasmid digested with HindIII served as positive control, and undigested plasmid served as negative control.

Activity of ZFNs on Genomic DNA: Southern Blot

L30 *lacZ*$^+$ fibroblasts were transfected with the ZFN plasmids using the Attractene Transfection Reagent (QIAGEN). After 8 or 18 hr, genomic DNA was isolated using the total DNA purification Kit (Epicenter). As positive control, 10 μg of L30 *lacZ*$^+$ genomic DNA was digested with HindIII for 2 hr at 37°C. 15 μg genomic DNA was loaded on a 1% agarose gel. The gel was incubated with 0.2 N HCl, denatured, neutralized, and transferred overnight on a Hybond nylon membrane (GE Healthcare) using 10× SSC buffer (pH 7). Membrane was auto-crosslinked with 2,400 mJ UV irradiation, pre-hybridized for 1 hr at 45°C with salmon sperm DNA and Roti-Hybriquick solution (Roth), and finally hybridized with the radioactive label (^{32}P-dCTP probe against bp 849–2,442) overnight at 48°C. After stringent washing, the membrane was exposed to a PhosphoImager screen and analyzed using AIDA Image Analyzer and ImageJ software. Radioactive-labeled probe was generated using the random primed DNA labeling Kit (NEB) according to the manufacturer's instructions.

Toxicity Assay

Toxicity assays were performed as previously described (Pruett-Miller et al., 2008). To calculate the percent survival relative to I-SceI, the ratio after nuclease transfection was normalized to the ratio after I-SceI transfection and this determined the percent survival compared to I-SceI.

Western Blot Analysis of ZFN and Chk2-Protein

Transduced cells were re-suspended in Mg^{2+} lysis/wash buffer (Upstate Cell Signaling Solutions) containing 10% glycerol, 25 mM sodium fluoride, 1 mM sodium orthovanadate, and a protease inhibitor cocktail (Roche Diagnostics), incubated for 15 min on ice, and centrifuged. Equal amounts of protein were used for western blot analysis. ZFN was visualized using anti-FLAG-tag antibody (OctA-Probe [D8]: sc-807, Santa Cruz). Chk2 and Chk2 KD were detected using anti-Chk2 antibody (sc-17747 [a-11], Santa Cruz), and anti-β-actin (Sigma) was used to determine total protein levels.

Isolation of BM and Retroviral Transduction

Lineage-negative cells from BM were pre-stimulated for 2 days in Iscove's modified Dulbecco's medium (IMDM; Lonza) supplemented with 10% fetal bovine serum (FBS), 1% penicillin/streptomycin, 2 mM L-glutamine, 50 ng/ml rat stem cell factor, 10 ng/ml mIL-3, 100 ng/mL mFlt3-ligand, and 100 ng/ml mIL-11 (Prospec) at a density of 6–8 × 10^6 cells/well. Viral transduction was performed on day 3 in RetroNectin-coated (TaKaRa) non-tissue culture plates that were preloaded with viral supernatant by centrifugation. Pre-stimulated BM cells were seeded on top (9–9.5 × 10^5 cells/well), and another layer of virus with cytokines was added. Media was changed the next morning, and another round of transduction was carried out overnight. The next day, cells were harvested using cell dissociation buffer (Gibco) and GFP+ cells were sorted by FACS on a BD FACS Aria II or III (BD Bioscience).

CFC Assay

CFC assays were performed as described elsewhere (Geiger et al., 2001; Xing et al., 2006).

Transplantation

For competitive transplantation, equal numbers (1–2 × 10^6) of young (2–4 months) $Ly5.1^+$ total BM cells and aged (18–24 months) $Ly5.2^+$ total BM cells were mixed and transplanted into lethally irradiated (11 Gy) $Ly5.1^+$ recipient mice. After 3 months, one cohort of transplanted mice (n = 7) was irradiated with 3 Gy. Ly5.2-chimerism in all hematopoietic compartments was investigated after 3 months (PB, BM, BM-HSPCs, spleen, spleen-HSPCs, and thymus) using flow cytometry. To investigate in vivo behavior of cells transduced with the ZFNs, 1–4 × 10^5 sorted GFP+ Lin^- cells in 200 μl PBS/mouse were transplanted into lethally irradiated (11 Gy) 3–6 months old BoyJ ($Ly5.1^+$) mice via retro-orbital injection. To determine effects of Chk2 overexpression and expression of Chk2 kinase-dead (KD), Ly 5.2^+ BM cells were transduced with the appropriate virus and equal numbers of cells were mixed with (1–2 × 10^6) $Ly5.1^+$ BM cells and transplanted into lethally irradiated $Ly5.1^+$ recipient mice. Peripheral blood (PB) chimerism was analyzed every 4 weeks by flow cytometry.

Flow Cytometry and Cell Sorting

For apoptosis and cell-cycle analyses, young (2–3 months) and aged (18–24 month) C57BL/6 mice were irradiated with 3 or 7 Gy (n = 4). After 16 hr, 500 μg BrdU (Becton Dickinson [BD], Cell Cycle Kit) in 200 μl PBS/mouse was injected intraperitoneally. After 45 min, the mice were sacrificed, BM flushed, and mononuclear cells isolated by low-density centrifugation. 2 × 10^6 cells were stained with a cocktail of biotinylated lineage antibodies after Fc block for 15 min: anti-Sca-1 (clone D7) (eBioscience), anti-c-Kit (clone ACK2) (eBioscience), anti-CD34 (clone RAM34) (eBioscience), and Streptavidin (eBioscience) for 1 hr on ice. Then cells were washed and incubated in 1× Binding Buffer (BD, Cell Cycle Kit) with anti-Annexin V antibody (BD, Apoptosis Detection Kit) for 20 min at RT. After washing cells were fixed and permeabilized using BD Cytofix/Cytoperm buffer (BD, Cell Cycle Kit). Cells were kept overnight in 1× permeabilization/washing buffer (BD, Cell Cycle Kit) and again permeabilized the next morning. Cells were then treated with 30 μg DNase (BD, Cell Cycle Kit) in PBS with Ca^{2+}/Mg^{2+} for 1.5 hr at 37°C and after washing incubated with anti-BrdU antibody (BD, Cell Cycle Kit) for 20 min at room temperature (RT). Finally, after washing, 7AAD was added and cells were immediately analyzed with a LSRII flow cytometer (BD Biosciences). LT-HSCs were defined as Lin^-/c-Kit^+/$Sca\text{-}1^+$/$CD34^{-/low}$, LSK represents Lin^-/c-Kit^+/$Sca\text{-}1^+$ cells, and hematopoietic progenitor cells were gated Lin^-/c-Kit^+. Apoptosis staining on Chk2 and Chk2 KD transduced c-Kit^+ BM cells was performed using the Annexin V antibody according to manufacturer's instructions (BD, Apoptosis Detection Kit). LT-HSCs were isolated as previously described (Florian et al., 2012).

8-oxo-dG Staining

Lineage-negative cells were harvested and incubated overnight at 37°C (5% CO_2, 3% O_2) in Hank's balanced salt solution (HBSS) supplemented with 10% FBS. After 16 hr cells were irradiated with 2 Gy and incubated for 1 hr at 37°C (5% CO_2, 3% O_2) in HBSS supplemented with 10% FBS. Then surface marker staining and permeabilization was completed as described in flow cytometry and cell sorting. Stained, fixed and permeabilized cells were incubated with 30 μg DNase I (BD, Cell Cycle Kit) in PBS with Ca^{2+}/Mg^{2+} for 1 hr at 37°C, washed, and stained overnight with the anti-8-oxo-dG antibody (clone 2E2, Trevigen). After 16 hr, cells were washed and stained with secondary antibody (Alexa 488 goat anti-mouse immunoglobulin G, Invitrogen).

Immunofluorescence Staining

Immunofluorescence staining was performed exactly as described previously (Florian et al., 2012).

Alkaline Comet Assay

LT-HSCs were incubated in IMDM medium (Lonza), 10% FBS, 1% penicillin/streptomycin, and 2 mM L-glutamine at 37°C (5% CO_2, 3% O_2) and irradiated the next day with 2 Gy (2 min 20 s at RT), put on ice, and centrifuged for 5 min at 1,500 rpm at RT. Cell were resuspended (zero time point) and incubated at 37°C (5% CO_2, 3% O_2) for 2 hr. Alkaline comet assay was performed with CometSlides and Comet Assay Reagent Kit (Trevigen). 1,000–1,500 LT-HSCs were encapsulated in 49 μl low-melting-point agarose on a pre-warmed CometSlide and incubated at 4°C in the dark for 30 min. Slides were immersed in 44 ml pre-chilled lysis solution (4 ml DMSO [Sigma] in 40 ml lysis solution) on ice for 40 min, drained of excess lysis solution, immersed into the alkaline solution for 30 min, and then placed into the electrophoresis chamber with alkaline buffer (pH = 13) at 4°C (30 V and 300 mA for 30 min). Excess buffer was drained, slides immersed twice in cold ddH_2O for 10 min, fixed by immersing in cold 70% ethanol for 5 min, and dried at 37°C for 30 min. For DNA staining, 100 μl diluted SYBR green 1 (1 μl 10,000× concentrated SYBR green 1 in 10 ml Tris-EDTA (TE) buffer (10 mM Tris-HCL [pH 7.5] and 1 mM EDTA) were added onto each sample. Cells were stained 5 min at 4°C before excess SYBR solution was removed. Dried slides were analyzed by fluorescence microscopy (Axio Observer Z1 microscope, Zeiss). Images of 50 cells of randomly chosen fields with equal exposure time were captured. Comet tail length and tail moment (%DNA in tail multiplied by tail length) were analyzed with the image analysis software CometScore (TriTek Corporation).

Statistical Analysis

Normal distribution of data was implied, and the variance between the groups was similar. Data are displayed as mean +1 SEM. All statistical analyses were performed using Student's t test with GraphPad Prism 6 software. In transplantation experiments, only healthy engrafted mice were included in analysis. For in vitro experiments, samples were excluded due to technical problems (procedure or reagents). The number of biological repeats (n) is indicated in figure legends.

SUPPLEMENTAL INFORMATION

Supplemental Information includes four figures and one table can be found with this article online at http://dx.doi.org/10.1016/j.celrep.2015.11.030.

AUTHOR CONTRIBUTIONS

B.M.M. and H.G. designed and interpreted experiments and wrote the manuscript. A.B., M.C.F., K.N., K.S., M.R., M.V., C.B., D.S., and D.W. performed and analyzed experiments. A.A., D.R.P., M.D.M., P.S., and M.P. assisted in designing and interpreting experiments.

ACKNOWLEDGMENTS

We thank Gary Van Zant and Jose A. Cancelas for advice and critical reading of the manuscript. We thank the cores at Ulm University and CCHMC for cell sorting support and the Comprehensive Mouse and Cancer Core at CCHMC for support with animal experiments. This work was supported by grants from the Deutsche Forschungsgemeinschaft (SFB 1079, KFO 142), The German Scholar Organization, the BMBF-funded Program SyStaR, the Edward P. Evans Foundation, and the National Institute of Health (HL076604, DK077762 and AG040118) to H.G. and a "Bausteinprogramm" of the Department of Medicine Ulm to M.C.F.

Received: June 30, 2015
Revised: August 13, 2015
Accepted: November 8, 2015
Published: December 10, 2015

REFERENCES

Aladjem, M.I., Spike, B.T., Rodewald, L.W., Hope, T.J., Klemm, M., Jaenisch, R., and Wahl, G.M. (1998). ES cells do not activate p53-dependent stress responses and undergo p53-independent apoptosis in response to DNA damage. Curr. Biol. *8*, 145–155.

Beerman, I., Seita, J., Inlay, M.A., Weissman, I.L., and Rossi, D.J. (2014). Quiescent hematopoietic stem cells accumulate DNA damage during aging that is repaired upon entry into cell cycle. Cell Stem Cell *15*, 37–50.

Boerrigter, M.E., Dollé, M.E., Martus, H.J., Gossen, J.A., and Vijg, J. (1995). Plasmid-based transgenic mouse model for studying in vivo mutations. Nature *377*, 657–659.

Bosco, E.E., and Knudsen, E.S. (2005). Differential role of RB in response to UV and IR damage. Nucleic Acids Res. *33*, 1581–1592.

Buschfort-Papewalis, C., Moritz, T., Liedert, B., and Thomale, J. (2002). Down-regulation of DNA repair in human CD34(+) progenitor cells corresponds to increased drug sensitivity and apoptotic response. Blood *100*, 845–853.

Cancer Genome Atlas Research Network (2013). Genomic and epigenomic landscapes of adult de novo acute myeloid leukemia. N. Engl. J. Med. *368*, 2059–2074.

Chambers, S.M., Shaw, C.A., Gatza, C., Fisk, C.J., Donehower, L.A., and Goodell, M.A. (2007). Aging hematopoietic stem cells decline in function and exhibit epigenetic dysregulation. PLoS Biol. *5*, e201.

Chute, J.P., Fung, J., Muramoto, G., and Erwin, R. (2004). Ex vivo culture rescues hematopoietic stem cells with long-term repopulating capacity following harvest from lethally irradiated mice. Exp. Hematol. *32*, 308–317.

Cousin, W., Ho, M.L., Desai, R., Tham, A., Chen, R.Y., Kung, S., Elabd, C., and Conboy, I.M. (2013). Regenerative capacity of old muscle stem cells declines without significant accumulation of DNA damage. PLoS ONE *8*, e63528.

Daria, D., Filippi, M.-D., Knudsen, E.S., Faccio, R., Li, Z., Kalfa, T., and Geiger, H. (2008). The retinoblastoma tumor suppressor is a critical intrinsic regulator for hematopoietic stem and progenitor cells under stress. Blood *111*, 1894–1902.

Deckbar, D., Jeggo, P.A., and Löbrich, M. (2011). Understanding the limitations of radiation-induced cell cycle checkpoints. Crit. Rev. Biochem. Mol. Biol. *46*, 271–283.

Di Leonardo, A., Linke, S.P., Clarkin, K., and Wahl, G.M. (1994). DNA damage triggers a prolonged p53-dependent G1 arrest and long-term induction of Cip1 in normal human fibroblasts. Genes Dev. *8*, 2540–2551.

Dignam, J.D., Lebovitz, R.M., and Roeder, R.G. (1983). Accurate transcription initiation by RNA polymerase II in a soluble extract from isolated mammalian nuclei. Nucleic Acids Res. *11*, 1475–1489.

Dollé, M.E., Giese, H., Hopkins, C.L., Martus, H.J., Hausdorff, J.M., and Vijg, J. (1997). Rapid accumulation of genome rearrangements in liver but not in brain of old mice. Nat. Genet. *17*, 431–434.

Dollé, M.E., Snyder, W.K., Gossen, J.A., Lohman, P.H., and Vijg, J. (2000). Distinct spectra of somatic mutations accumulated with age in mouse heart and small intestine. Proc. Natl. Acad. Sci. USA *97*, 8403–8408.

Flach, J., Bakker, S.T., Mohrin, M., Conroy, P.C., Pietras, E.M., Reynaud, D., Alvarez, S., Diolaiti, M.E., Ugarte, F., Forsberg, E.C., et al. (2014). Replication stress is a potent driver of functional decline in ageing haematopoietic stem cells. Nature *512*, 198–202.

Florian, M.C., Dörr, K., Niebel, A., Daria, D., Schrezenmeier, H., Rojewski, M., Filippi, M.-D., Hasenberg, A., Gunzer, M., Scharffetter-Kochanek, K., et al. (2012). Cdc42 activity regulates hematopoietic stem cell aging and rejuvenation. Cell Stem Cell *10*, 520–530.

Geiger, H., True, J.M., de Haan, G., and Van Zant, G. (2001). Age- and stage-specific regulation patterns in the hematopoietic stem cell hierarchy. Blood *98*, 2966–2972.

Geiger, H., Schleimer, D., Nattamai, K.J., Dannenmann, S.R., Davies, S.M., and Weiss, B.D. (2006). Mutagenic potential of temozolomide in bone marrow cells in vivo. Blood *107*, 3010–3011.

Please cite this article in press as: Moehrle et al., Stem Cell-Specific Mechanisms Ensure Genomic Fidelity within HSCs and upon Aging of HSCs, Cell Reports (2015), http://dx.doi.org/10.1016/j.celrep.2015.11.030

Geiger, H., David, S., Nattamai, K.J., and Jan, V. (2009). Quantification of genomic mutations in murine hematopoietic cells. Methods Mol. Biol. *506*, 423–436.

Geiger, H., de Haan, G., and Florian, M.C. (2013). The ageing haematopoietic stem cell compartment. Nat. Rev. Immunol. *13*, 376–389.

Genovese, G., Kähler, A.K., Handsaker, R.E., Lindberg, J., Rose, S.A., Bakhoum, S.F., Chambert, K., Mick, E., Neale, B.M., Fromer, M., et al. (2014). Clonal hematopoiesis and blood-cancer risk inferred from blood DNA sequence. N. Engl. J. Med. *371*, 2477–2487.

Hérodin, F., and Drouet, M. (2005). Cytokine-based treatment of accidentally irradiated victims and new approaches. Exp. Hematol. *33*, 1071–1080.

Hirao, A., Kong, Y.Y., Matsuoka, S., Wakeham, A., Ruland, J., Yoshida, H., Liu, D., Elledge, S.J., and Mak, T.W. (2000). DNA damage-induced activation of p53 by the checkpoint kinase Chk2. Science *287*, 1824–1827.

Hong, Y., and Stambrook, P.J. (2004). Restoration of an absent G1 arrest and protection from apoptosis in embryonic stem cells after ionizing radiation. Proc. Natl. Acad. Sci. USA *101*, 14443–14448.

Inomata, K., Aoto, T., Binh, N.T., Okamoto, N., Tanimura, S., Wakayama, T., Iseki, S., Hara, E., Masunaga, T., Shimizu, H., and Nishimura, E.K. (2009). Genotoxic stress abrogates renewal of melanocyte stem cells by triggering their differentiation. Cell *137*, 1088–1099.

Insinga, A., Cicalese, A., Faretta, M., Gallo, B., Albano, L., Ronzoni, S., Furia, L., Viale, A., and Pelicci, P.G. (2013). DNA damage in stem cells activates p21, inhibits p53, and induces symmetric self-renewing divisions. Proc. Natl. Acad. Sci. USA *110*, 3931–3936.

Ito, K., Hirao, A., Arai, F., Matsuoka, S., Takubo, K., Hamaguchi, I., Nomiyama, K., Hosokawa, K., Sakurada, K., Nakagata, N., et al. (2004). Regulation of oxidative stress by ATM is required for self-renewal of haematopoietic stem cells. Nature *431*, 997–1002.

Kastan, M.B., and Bartek, J. (2004). Cell-cycle checkpoints and cancer. Nature *432*, 316–323.

Krejci, O., Wunderlich, M., Geiger, H., Chou, F.-S., Schleimer, D., Jansen, M., Andreassen, P.R., and Mulloy, J.C. (2008). p53 signaling in response to increased DNA damage sensitizes AML1-ETO cells to stress-induced death. Blood *111*, 2190–2199.

Kushner, B.H., Laquaglia, M.P., Kramer, K., Modak, S., and Cheung, N.-K.V. (2008). Recurrent metastatic neuroblastoma followed by myelodysplastic syndrome: possible leukemogenic role of temozolomide. Pediatr. Blood Cancer *51*, 552–554.

Lee, H.W., Blasco, M.A., Gottlieb, G.J., Horner, J.W., 2nd, Greider, C.W., and DePinho, R.A. (1998). Essential role of mouse telomerase in highly proliferative organs. Nature *392*, 569–574.

Li, M., He, Y., Dubois, W., Wu, X., Shi, J., and Huang, J. (2012). Distinct regulatory mechanisms and functions for p53-activated and p53-repressed DNA damage response genes in embryonic stem cells. Mol. Cell *46*, 30–42.

Linton, P.J., and Dorshkind, K. (2004). Age-related changes in lymphocyte development and function. Nat. Immunol. *5*, 133–139.

Liu, L., Cheung, T.H., Charville, G.W., Hurgo, B.M.C., Leavitt, T., Shih, J., Brunet, A., and Rando, T.A. (2013). Chromatin modifications as determinants of muscle stem cell quiescence and chronological aging. Cell Rep. *4*, 189–204.

Maeder, M.L., Thibodeau-Beganny, S., Sander, J.D., Voytas, D.F., and Joung, J.K. (2009). Oligomerized pool engineering (OPEN): an 'open-source' protocol for making customized zinc-finger arrays. Nat. Protoc. *4*, 1471–1501.

Mohrin, M., Bourke, E., Alexander, D., Warr, M.R., Barry-Holson, K., Le Beau, M.M., Morrison, C.G., and Passegué, E. (2010). Hematopoietic stem cell quiescence promotes error-prone DNA repair and mutagenesis. Cell Stem Cell *7*, 174–185.

Nakamura, A.J., Chiang, Y.J., Hathcock, K.S., Horikawa, I., Sedelnikova, O.A., Hodes, R.J., and Bonner, W.M. (2008). Both telomeric and non-telomeric DNA damage are determinants of mammalian cellular senescence. Epigenetics Chromatin *1*, 6.

Navarro, S., Meza, N.W., Quintana-Bustamante, O., Casado, J.A., Jacome, A., McAllister, K., Puerto, S., Surrallés, J., Segovia, J.C., and Bueren, J.A. (2006). Hematopoietic dysfunction in a mouse model for Fanconi anemia group D1. Mol. Ther. *14*, 525–535.

Nijnik, A., Woodbine, L., Marchetti, C., Dawson, S., Lambe, T., Liu, C., Rodrigues, N.P., Crockford, T.L., Cabuy, E., Vindigni, A., et al. (2007). DNA repair is limiting for haematopoietic stem cells during ageing. Nature *447*, 686–690.

Noronha, V., Berliner, N., Ballen, K.K., Lacy, J., Kracher, J., Baehring, J., and Henson, J.W. (2006). Treatment-related myelodysplasia/AML in a patient with a history of breast cancer and an oligodendroglioma treated with temozolomide: case study and review of the literature. Neuro-oncol. *8*, 280–283.

Parmar, K., Kim, J., Sykes, S.M., Shimamura, A., Stuckert, P., Zhu, K., Hamilton, A., Deloach, M.K., Kutok, J.L., Akashi, K., et al. (2010). Hematopoietic stem cell defects in mice with deficiency of Fancd2 or Usp1. Stem Cells *28*, 1186–1195.

Pietras, E.M., Warr, M.R., and Passegué, E. (2011). Cell cycle regulation in hematopoietic stem cells. J. Cell Biol. *195*, 709–720.

Porteus, M. (2008). Design and testing of zinc finger nucleases for use in mammalian cells. Methods Mol. Biol. *435*, 47–61.

Porteus, M.H., and Baltimore, D. (2003). Chimeric nucleases stimulate gene targeting in human cells. Science *300*, 763.

Prasher, J.M., Lalai, A.S., Heijmans-Antonissen, C., Ploemacher, R.E., Hoeijmakers, J.H., Touw, I.P., and Niedernhofer, L.J. (2005). Reduced hematopoietic reserves in DNA interstrand crosslink repair-deficient Ercc1-/- mice. EMBO J. *24*, 861–871.

Pruett-Miller, S.M., Connelly, J.P., Maeder, M.L., Joung, J.K., and Porteus, M.H. (2008). Comparison of zinc finger nucleases for use in gene targeting in mammalian cells. Mol. Ther. *16*, 707–717.

Reese, J.S., Liu, L., and Gerson, S.L. (2003). Repopulating defect of mismatch repair-deficient hematopoietic stem cells. Blood *102*, 1626–1633.

Rossi, D.J., Bryder, D., Seita, J., Nussenzweig, A., Hoeijmakers, J., and Weissman, I.L. (2007a). Deficiencies in DNA damage repair limit the function of haematopoietic stem cells with age. Nature *447*, 725–729.

Rossi, D.J., Seita, J., Czechowicz, A., Bhattacharya, D., Bryder, D., and Weissman, I.L. (2007b). Hematopoietic stem cell quiescence attenuates DNA damage response and permits DNA damage accumulation during aging. Cell Cycle *6*, 2371–2376.

Rübe, C.E., Fricke, A., Widmann, T.A., Fürst, T., Madry, H., Pfreundschuh, M., and Rübe, C. (2011). Accumulation of DNA damage in hematopoietic stem and progenitor cells during human aging. PLoS ONE *6*, e17487.

Ruzankina, Y., Pinzon-Guzman, C., Asare, A., Ong, T., Pontano, L., Cotsarelis, G., Zediak, V.P., Velez, M., Bhandoola, A., and Brown, E.J. (2007). Deletion of the developmentally essential gene ATR in adult mice leads to age-related phenotypes and stem cell loss. Cell Stem Cell *1*, 113–126.

Sancar, A., Lindsey-Boltz, L.A., Unsal-Kaçmaz, K., and Linn, S. (2004). Molecular mechanisms of mammalian DNA repair and the DNA damage checkpoints. Annu. Rev. Biochem. *73*, 39–85.

Schuler, N., and Rübe, C.E. (2013). Accumulation of DNA damage-induced chromatin alterations in tissue-specific stem cells: the driving force of aging? PLoS ONE *8*, e63932.

Shao, L., Feng, W., Li, H., Gardner, D., Luo, Y., Wang, Y., Liu, L., Meng, A., Sharpless, N.E., and Zhou, D. (2014). Total body irradiation causes long-term mouse BM injury via induction of HSC premature senescence in an Ink4a- and Arf-independent manner. Blood *123*, 3105–3115.

Signer, R.A.J., and Morrison, S.J. (2013). Mechanisms that regulate stem cell aging and life span. Cell Stem Cell *12*, 152–165.

Su, Y.-W., Chang, M.-C., Chiang, M.-F., and Hsieh, R.-K. (2005). Treatment-related myelodysplastic syndrome after temozolomide for recurrent high-grade glioma. J. Neurooncol. *71*, 315–318.

van Harn, T., Foijer, F., van Vugt, M., Banerjee, R., Yang, F., Oostra, A., Joenje, H., and te Riele, H. (2010). Loss of Rb proteins causes genomic instability in the absence of mitogenic signaling. Genes Dev. *24*, 1377–1388.

Van Zant, G., and Liang, Y. (2012). Concise review: hematopoietic stem cell aging, life span, and transplantation. Stem Cells Transl. Med. *1*, 651–657.

Vijg, J., Dollé, M.E., Martus, H.J., and Boerrigter, M.E. (1997). Transgenic mouse models for studying mutations in vivo: applications in aging research. Mech. Ageing Dev. *99*, 257–271.

Wang, J., Sun, Q., Morita, Y., Jiang, H., Gross, A., Lechel, A., Hildner, K., Guachalla, L.M., Gompf, A., Hartmann, D., et al. (2012). A differentiation checkpoint limits hematopoietic stem cell self-renewal in response to DNA damage. Cell *148*, 1001–1014.

Welch, J.S., Ley, T.J., Link, D.C., Miller, C.A., Larson, D.E., Koboldt, D.C., Wartman, L.D., Lamprecht, T.L., Liu, F., Xia, J., et al. (2012). The origin and evolution of mutations in acute myeloid leukemia. Cell *150*, 264–278.

Xing, Z., Ryan, M.A., Daria, D., Nattamai, K.J., Van Zant, G., Wang, L., Zheng, Y., and Geiger, H. (2006). Increased hematopoietic stem cell mobilization in aged mice. Blood *108*, 2190–2197.

Zhang, Q.-S., Marquez-Loza, L., Eaton, L., Duncan, A.W., Goldman, D.C., Anur, P., Watanabe-Smith, K., Rathbun, R.K., Fleming, W.H., Bagby, G.C., and Grompe, M. (2010). Fancd2-/- mice have hematopoietic defects that can be partially corrected by resveratrol. Blood *116*, 5140–5148.